



Ionosonde Total Electron Content Evaluation Using IGS Data

Telmo dos Santos Klipp¹, Adriano Petry¹, Gabriel Sandim Falcão¹, Jonas Rodrigues de Souza², Eurico Rodrigues de Paula², and Haroldo Fraga de Campos Velho²

¹National Institute for Space Research, Southern Regional Space Research Center, Av Roraima, campus UFSM, prédio do INPE/CRS, sala 2023, PO box 5021, zipcode 97105-970, Santa Maria, RS, Brazil, Phone: +55 55 33012012.

²National Institute for Space Research, Av. dos Astronautas, 1758 - Jardim da Granja, São José dos Campos/SP - CEP 12227-010 - Brasil.

Correspondence: Telmo dos Santos Klipp (telmo.klipp@gmail.com)

Abstract. In this work, a period of two years (2016-2017) of vertical total electron content (VTEC) from ionosondes operating in Brazil is compared to the International GNSS Service (IGS) data. Sounding instruments from National Institute for Space Research (INPE) provided the ionograms used, which were filtered based on confidence score (CS) and C-level flags evaluation. Differences between TEC from IGS maps and ionograms were accumulated in terms of root mean square error (RMSE). It has been noticed the TEC values provided by ionograms are systematically underestimated, which is attributed to a limitation in the electron density modeled for the ionogram topside that considers maximum height only around 800-900 Km, while IGS takes in account electron density from GNSS stations up to the satellite network orbits. The ionogram topside profiles covering the plasmasphere were re-modeled using an adaptive α -Chapman exponential decay that includes a transition function between the F2 layer and plasmasphere, and electron density integration height was extended to compute TEC. Chapman parameters for the F2 layer were extracted from each ionogram, and plasmaspheric scale height was set to 10,000 Km. Our analysis has shown the plasmaspheric basis electron density, assumed to be proportional to the electron peak density, plays an important role to reduce the RMSE values. Depending on the proportionality coefficient choice, mean RMSE reached a minimum of 5.32 TECU, that is 23% lower than initial ionograms TEC errors.

1 Introduction

The understanding of ionospheric behaviour provides important information about the space weather. In addition, the total electron content (TEC) affects group and phase delays of radio waves passing through ionosphere and impacts, among other, global navigation satellite systems (GNSS). Different instruments are capable of evaluating electron density in ionosphere, and validations among different sources of data can lead to interesting conclusions. While ionosonde instruments provide "ground truth" measures for the bottom side of ionospheric profile and estimate the topside using exponential decay function, ground GNSS stations receiving radio signals from orbiting satellites can provide large scale details of the entire ionosphere structure



and even plasmasphere (Huang and Reinisch, 2001; Reinisch and Huang, 2001; Jakowski, 2005; Reinisch and Galkin, 2011; Jin and Jin, 2011). The analysis proposed in this work is based on comparisons between TEC estimated using ionograms, and from the International GNSS Service (IGS). While IGS has its own intrinsic quality control through a ranking system (Hernández-Pajares et al., 2009), ionosonde data is evaluated by its auto-scaling system, and quality scores are assigned to each ionogram. The study was performed in Brazilian region for a 2-year period (2016-2017), where ionosonde data from National Institute for Space Research (INPE) were available. Indeed, the plasmaspheric electron density has been considered using an adapted α -Chapman function (Jakowski, 2005), and the adjustment in the plasmaspheric basis electron density was based on differences to IGS data.

1.1 IGS VTEC maps

IGS vertical total electron content (VTEC) maps is considered to be a reliable ionospheric information product, which was achieved from integrating scientific community efforts (Hernández-Pajares et al., 2009). Such maps are generated by a combination of data from different research institutions within a method that is based on ranking different VTEC maps to compose the final product (Hernández-Pajares et al., 2009). The process begins with raw data from the GNSS ground network being acquired and sent to ionospheric associate analysis centers (IAACs) so the VTEC maps can be generated using the ionosphere map exchange (IONEX) format (Schaer et al., 1998). To achieve a high level of quality, these VTEC maps are evaluated, and its ability to reproduce corresponding slant TEC (STEC) maps is checked. Next, a combination process takes place using a weighted mean of the VTEC maps available. The final step before making the maps available for access on the IGS server is a validation process. It compares the VTEC maps to an independent source: dual frequency altimeters on board TOPEX, JASON and ENVISAT satellites.

1.2 Ionosonde data

An ionosonde measures the returning echoes of pulse signals at a fixed location to estimate ionospheric characteristics and to produce a vertical electron density profile (ionogram). The bottom side profile starts with measures at ~ 90 km up to the peak of the F2 layer (f_0F_2), around 350 km. The ionosphere topside profile, instead, is modeled using an exponential decay function. The integration of electron density in height produces an estimate for the TEC value.

Ionograms can be interpreted either manually by expert or automatically using software. The autoscaling ionosonde data availability, rather than manual scaling, contributes to meet practical applications (Jiang et al., 2015). Different systems were created and concentrated efforts have been applied to improve autoscaling (Reinisch and Xueqin, 1983; Scotto and Pezzopane, 2002, 2007; Reinisch et al., 2005). Also, a standard archiving output (SAO) format was created by initiative of the Ionospheric Informatics Working Group (IIWG) to store and disseminate auto-scaled data. Initially, SAO format considered only ionograms scaled by automatic real-time ionogram scaler with true height (ARTIST), however, it evolved to hold scaled data from others sounder systems (Galkin, 2006).



1.2.1 Ionogram quality

Several attempts had been made to verify ionogram quality (Reinisch et al., 2005). Stankov et al. (2012) investigated over 60,000 soundings generated by a digisonde using auto-scaling system ARTIST 4 for the period of 2002 to 2008 and corresponding manually scaled data from experienced scalers. They found out that seasonal and diurnal variation led to overestimation or underestimation of ionospheric characteristics. Residual errors between manually and auto-scaled values pointed to improvements to be made when facing weak or gaped echoes traces. These problems were related and faced in Reinisch et al. (2005). Pezzopane and Scotto (2007) made a comparison between ARTIST 4.5 and AUTOSCALA systems. According to them, ARTIST 4.5 faces problems not only when dealing with weak or gaped traces, but also with information from wave polarization. So far, automatic extraction of ionospheric characteristics results in $\sim 5\%$ of ionograms ranked as unscalable. Further improvements in ARTIST 5 deals with such problems as reported in (Galkin and Reinisch, 2008). Also, quiet geomagnetic conditions tend to improve auto-scaling results and reduce scaling processing challenges (Stankov et al., 2012; Pezzopane and Scotto, 2007).

Ionosonde data scaled by ARTIST 5 have a quality metric called confidence score (CS). Such metric is based on quality criteria supported by concepts of ionogram interpretation and algorithms that specify the uncertainty and confidence of scaled results (Galkin et al., 2013). The CS metric includes quality checking solutions introduced by confidence calculation schemes developed since late 1980s: the auto-scaling confidence level (ACL) quality flag, the two-digit confidence level (C-Level) and the QUALSCAN quality control (Galkin et al., 2013). The estimation of confidence score occurs during ionogram processing. Ionogram interpretation criteria consider not only analysis of extracted trace shapes, but ionospheric conditions to compute per-point-error reduction. The CS starts with a value of 100. If an interpretation criteria is found, its per-point-error value is subtracted from CS. To be considered acceptable for further use, auto-scaling records need to reach a CS above a predefined threshold value, which is generally 40 (Galkin et al., 2013).

The SAO format version 4 does not have the CS on its specifications, but have the C-Level representation. The two digits range goes from 11 (highest confidence) to 55 (lowest confidence). The CS produced by ARTIST 5 can be converted to C-Level representation using the Table 1 (Galkin et al., 2013).

2 Methodology

Ionosonde data was obtained from INPE database using files in SAO format (version 4) and scaled by auto-scaling system ARTIST (version 5). Data from up to 5 instruments (see Fig. 1) were available at the same time for the period considered (2016-2017). Although ionosondes can generate ionograms in less than ten minutes interval, a 1 hour interval between soundings was considered in this work, except for the comparisons with IGS data. In that case, 2 hours interval is used to match IGS data availability.



Figure 1. Location of available ionosonde data during 2016-2017.

C-Level values were extracted from all ionograms, and despite auto-scaled ionosonde data with CS above 40 can be considered acceptable (Galkin et al., 2013), we chose to use only those achieving a CS above 60, corresponding to C-level 11 and 22. Figure 2 shows the total number of C-Level flags occurrences for the available data. Figure 3 shows the same distribution, however, considering each ionosonde station separately. It can be seen from Fig. 2 and 3 that the majority of C-Level flags occurrences are in classification levels 11 or 22. Also, more than half of C-Level flags achieve CS above 80 (C-level 11).

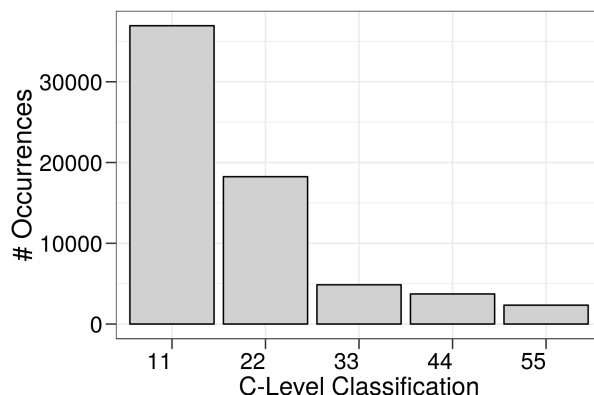


Figure 2. Distribution of C-Level flags for ionograms during 2016-2017.

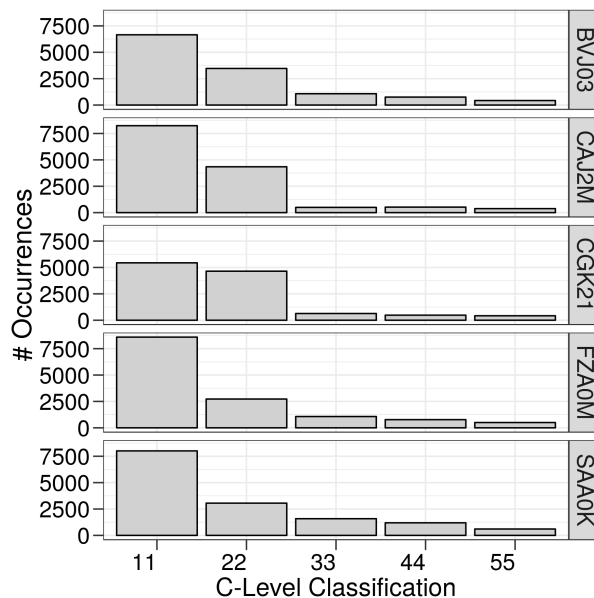


Figure 3. The same as Fig. 2 but for each ionosonde station separately.

Considering the daily variation in ionosphere electron density, it would be interesting to analyse also the ionosondes' data quality variation with the day hours taking into account all available data. It can be seen in Fig. 4 the increase in the occurrence of level 11 after sunset while the level 22 decreases. The aggregation of C-level flags 11 and 22 ionograms (used in this work) provides ionosonde data with over 1000 samples even for the period with low occurrences.

- TEC values from IGS maps and ionosondes were compared at the same date/time using the closest geographic correspondence as shown in Table 2, considering IGS data grid (5° in longitude per 2.5° in latitude, every 2 hours). The analysis is



mainly based on the accumulation of TEC differences by applying the root mean squared error (RMSE) as defined in Eq. (1) (Chai and Draxler, 2014):

$$RMSE = \sqrt{\frac{1}{n} \sum_{i=1}^n e_i^2} \quad (1)$$

where error e is the differences ($e_i, i=1,2,\dots,n$) between TEC values, and n is the total number of values considered.

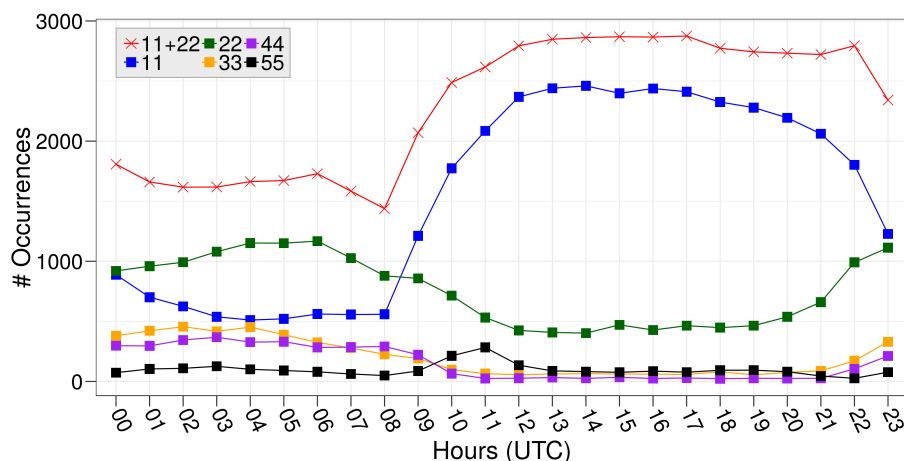


Figure 4. Hourly distribution of C-level flags.

5 3 Experiments and results

TEC daily variability for each ionosonde C-level flag is shown in Fig. 5, and for each ionosonde station separately, considering only C-level flags 11 and 22, is shown in Fig. 6. Since the daily mean TEC values from flags 11 and 22 follow the IGS data variation, they are coherent. Such coherence has been well explained by Klipp et al. (2019). These authors have analyzed the IGS TEC for the equatorial, low and mid latitudes and also for the same period as presented in this work. It was noticed seasonal
 10 TEC dependence with maxima during equinoxes for equatorial and low latitude sectors, but modulated by an overlay effect of the solar flux. On the other hand, it can be seen the TEC values from IGS are consistently higher than ionosondes for the whole period and for every ionosonde. It is also noticeable in Fig. 5, a noisy and incoherent TEC variation for flags greater than 22 in both ionosonde and the correspondent IGS data. Obviously, since the results for flags greater than 22 have low confidence, they may have errors, but this reason can not be used to explain the noise in IGS TEC values. The data representative for higher
 15 flags is low, i.e., there is reduced number of points and heterogeneous distribution during day and nighttime. Such unbalanced distribution can produce mean TEC representing only day or nighttime, that during consecutive days lead to noisy curves.

In Fig. 6 we can observe that some ionosondes presented lack of data for few days or even entire months. The seasonal variation in TEC was similar for all stations. During autumn and winter seasons in southern hemisphere we can notice a decrease in TEC values for both years evaluated.

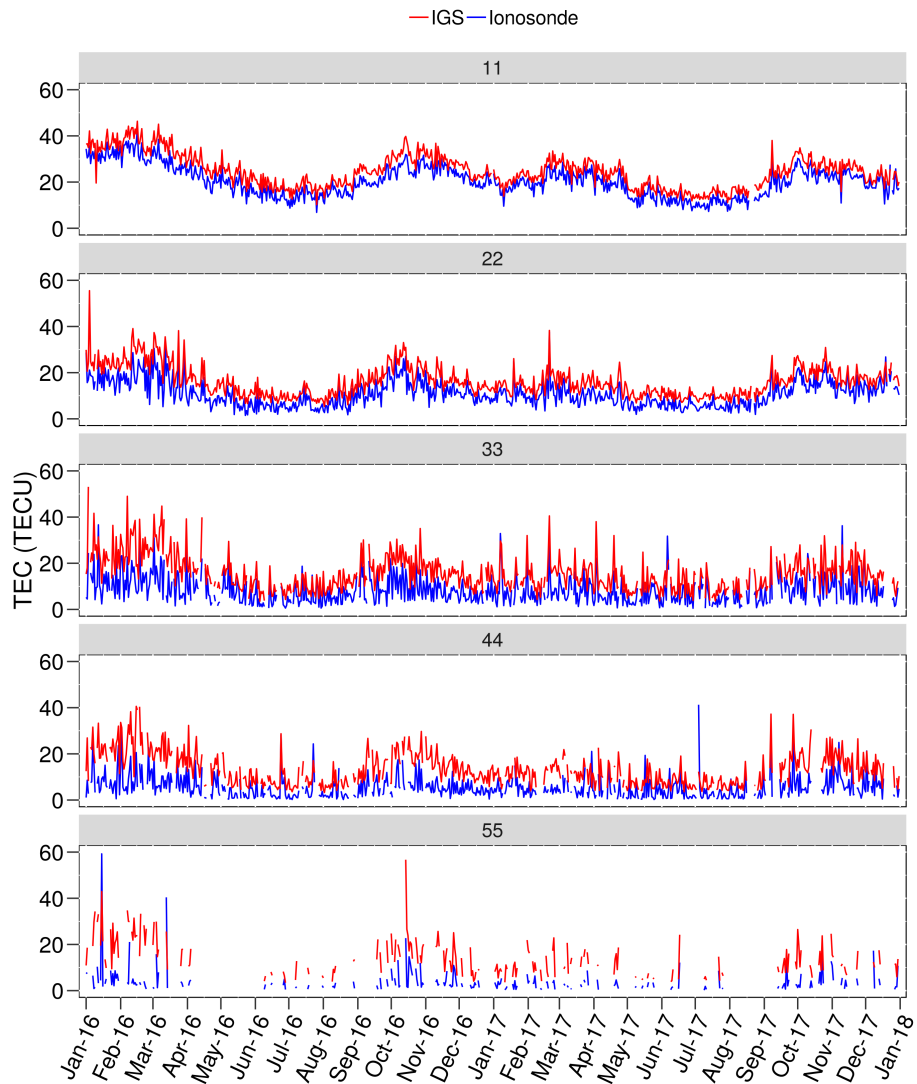


Figure 5. TEC daily variation for the period under analysis considering the mean value for each C-level flag classification.

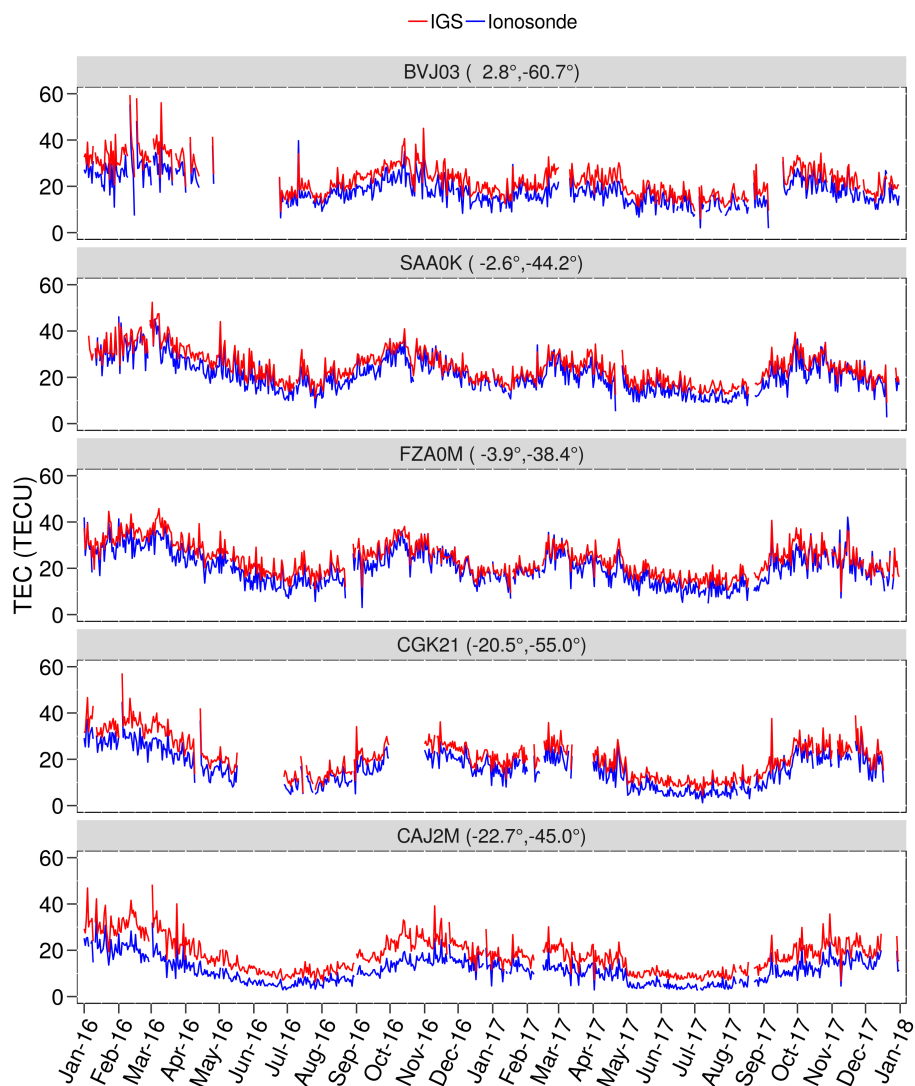


Figure 6. The same as Fig. 5 but considering only C-level flags 11 and 22 and for each ionosonde station separately.

Figure 7 (a) presents the daily accumulated TEC RMSE when comparing IGS and ionosondes. The seasonal variability in TEC differences seems highly correlated to ionization distribution along the analysed period. Figure 7 (b) shows the ionosondes peak of plasma frequency (f_0F_2), and we can observe the periods of high f_0F_2 values correspond to high RMSE. The maximum height used for electron density integration in ionosondes (Fig. 7 (c)) does not change significantly, rarely reaching 900 Km. Figure 7 (d) shows the plasma frequency at maximum altitude, which indicates the level from where it is necessary an extension of ionosphere structure evaluation to higher altitudes. Such contribution has not been included in the ionosonde TEC calculation. This is the main reason why the ionospheric TEC values from ionosondes are underestimated when compared to



IGS values. It is well known that TEC values from the IGS data represent the integrated electron density along the signal path between the receiver and the satellite altitude ($\sim 22,000$ Km). Thus, this analysis is in agreement with what is shown in Fig. 5 and 6.

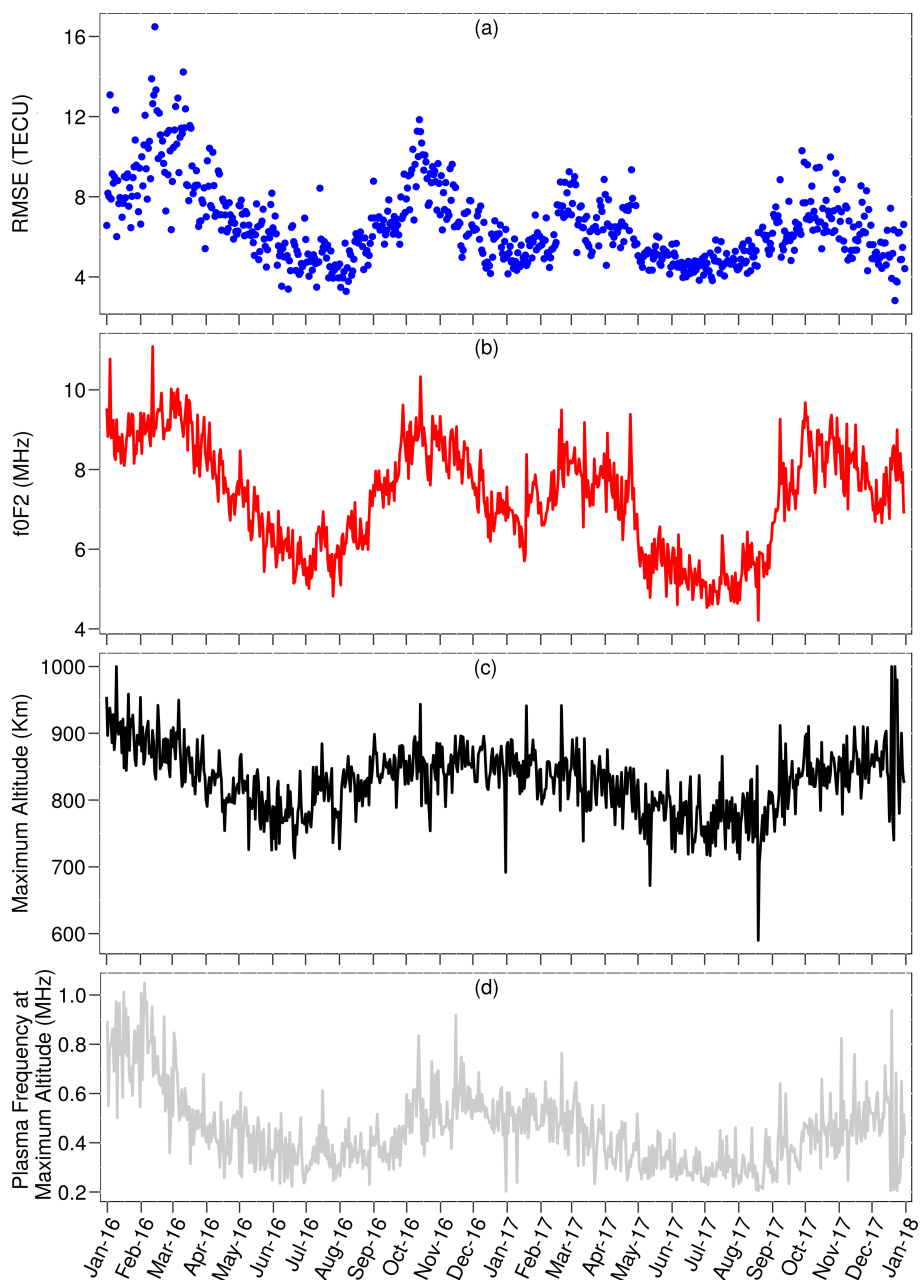


Figure 7. Ionosonde data: (a) TEC difference to IGS in terms of RMSE; (b) F2 layer critical frequency; (c) ionogram maximum altitude and (d) plasma frequency at maximum altitude.



To evaluate the discrepancies between IGS and ionosonde TEC, the ionograms topside profiles were re-modeled using an adapted α -Chapman exponential decay that includes a transition function between the F2 layer and plasmasphere. The adapted α -Chapman introduced by Jakowski (2005), defines the topside profile N_T as

$$N_T(h) = NmF2 \cdot \exp\left(\frac{1}{2}(1 - z - e^{-z})\right) + N_{P0} \cdot \exp\left(\frac{-h}{H_p}\right), \quad \text{where } z = \frac{h - hmF2}{H_T} \quad (2)$$

- 5 The ionograms provided F2 scale height H_T , the electron peak density $NmF2$ that can be derived from measured critical frequency f_0F2 using $NmF2 = (1/80.6) \cdot (f_0F2)^2$, and peak height $hmF2$. According to Jakowski (2005), the plasmaspheric scale height H_p can be defined as 10,000 km and the plasmaspheric basis density N_{P0} is assumed to be proportional to $NmF2$, i.e., $N_{P0} = K \cdot NmF2$. Using the topside reconstruction of ionograms shown above, the maximum integration height used to estimate ionosonde TEC values was defined as 20,000 Km, corresponding to an approximation for the satellites orbit.
- 10 Different values for the proportionality coefficient K were examined, and Fig. 8 shows the correspondent TEC differences to IGS in terms of total RMSE. When K is set to zero, Eq. (2) is reduced to regular α -Chapman decay, and plasmaspheric slowly decaying exponential term is ignored. As K increases, the underestimated ionosonde TEC values move closer to IGS, hence reducing RMSE. However, after an optimal K , in this experiment equals to $1/175$, the plasmaspheric contribution is exceeded, increasing again RMSE. The top panel of Fig. 9 compares the IGS daily mean TEC variation (in red), initial ionograms TEC
- 15 (in blue), and using adapted α -Chapman for ionogram topside reconstruction (in black), where we can notice a significant improvement in ionosonde fit to IGS data when the adapted α -Chapman is used. Bottom panel of Fig. 9 shows the RMSE variation using adapted α -Chapman (black triangle), compared to the initial ionogram errors as shown in Fig. 7 (a).

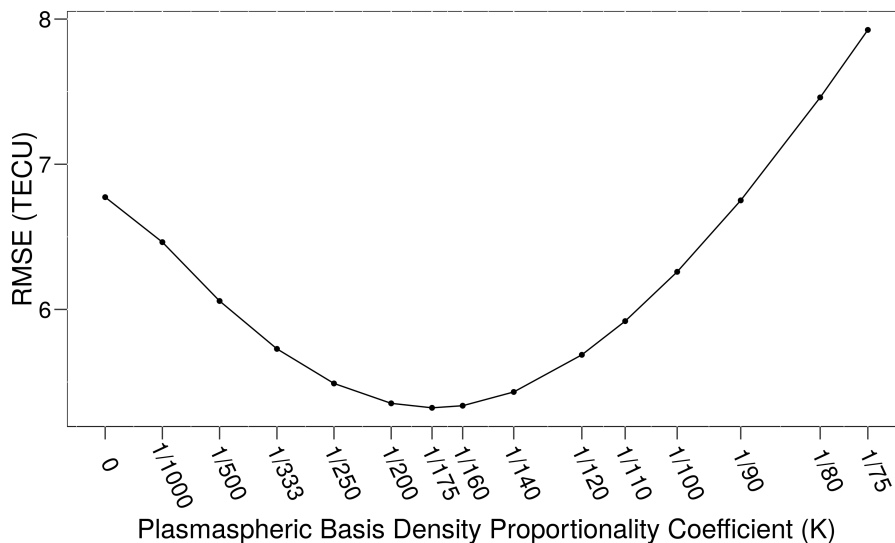


Figure 8. Variation of total RMSE with plasmaspheric basis density proportionality coefficient.

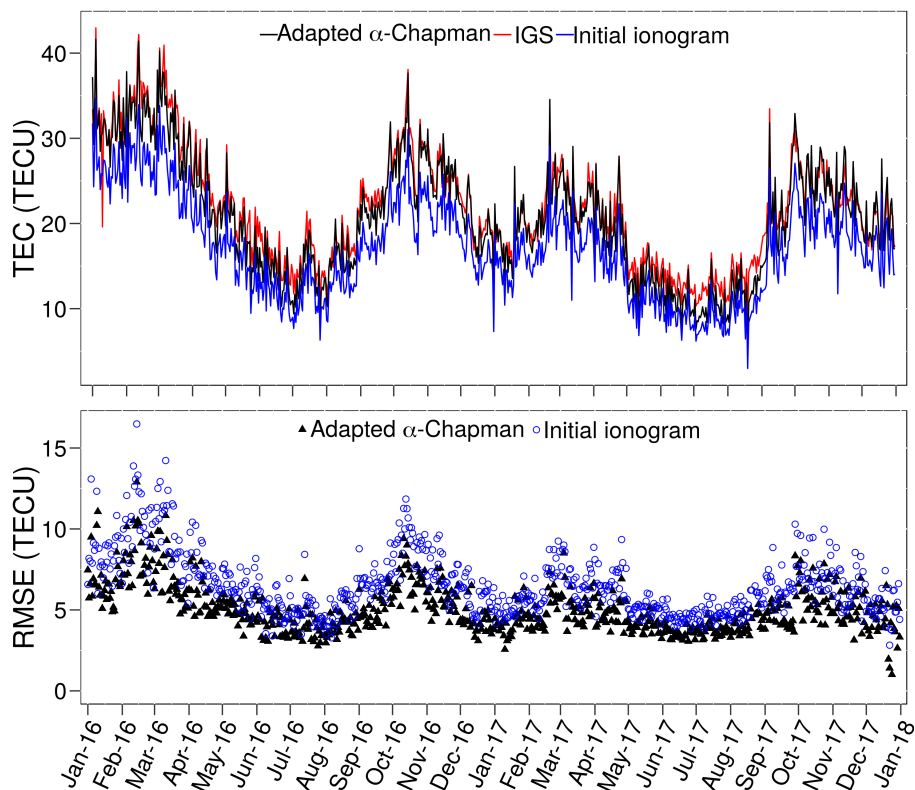


Figure 9. Top panel: Comparison of daily mean TEC for IGS (red), initial ionograms (blue) and using adapted α -Chapman for ionograms topside reconstruction (black). Bottom panel: RMSE variation using initial ionograms errors (blue circle) and adapted α -Chapman (black triangle).

4 Conclusions

This paper presented a 2-year period validation of ionosonde data, using IGS VTEC as reference. Ionogram electron density profiles were first selected based on the Confidence Score, and then integrated in height. We have noticed ionosonde TEC values were systematically underestimated, what is consistent to ionospheric topside modeling limitation that considers maximum height around 800-900 Km, while IGS data considers electron densities from the GNSS stations to the satellite altitudes. This claim was supported by the examination of Fig. 5 and 7. The ionogram topside profiles were re-modeled using an adapted α -Chapman exponential decay, and electron density integration height was extended to an approximation of satellites orbit. Hence, the plasmaspheric ionization contribution brought ionosonde TEC values closer to IGS observations. In fact, the vertical electron density distribution in the plasmasphere was determined based on adjustment of plasmaspheric basis density using an optimal factor (K) which minimizes the global RMSE. In our experiments, the improvement was significant, as shown in Fig. 9. Yet, we could observe the matching between ionosonde and IGS TEC seems worse during low ionization periods, mainly



nearby June solstice, what indicates the need of seasonal and solar cycle optimization for the plasmaspheric parameters. Such investigation will be done in a future work.

Competing interests. The authors declare that they have no conflict of interest.

Acknowledgements. T. S. Klipp would like to acknowledge Conselho Nacional de Desenvolvimento Científico e Tecnológico (CNPq, Brazil)

5 for Programa de Capacitação Institucional PCI-DC research sponsorship.

G. S. Falcão would like to acknowledge CNPq for PIBIC sponsorship.

J. R. Souza and E. R. Paula would like to thank the CNPq (under the respective grants 307181/2018-9 and 310802/2015-6) for research productivity sponsorship and the INCT GNSS-NavAer supported by CNPq (465648/2014-2), FAPESP (2017/50115-0) and CAPES (88887.137186/2017-00).

10 H. F. C. Velho would like to acknowledge CNPq for research productivity sponsorship.

The authors would like to acknowledge the Crustal Dynamics Data Information System (CDDIS), NASA Goddard Space Flight Center, Greenbelt, MD, USA for providing online access to IGS VTEC data at <ftp://cddis.gsfc.nasa.gov/gnss/products/ionex/igsg>.



References

- Chai, T. and Draxler, R. R.: Root mean square error (RMSE) or mean absolute error (MAE)? – Arguments against avoiding RMSE in the literature, *Geosci. Model Dev.*, 7, 1247–1250, <https://doi.org/10.5194/gmd-7-1247-2014>, 2014.
- Galkin, I., Reinisch, B. W., Huang, X., and Khmyrov, G. M.: Confidence Score of ARTIST-5 Ionogram Autoscaling, Tech. rep.,
5 Ionosonde Network Advisory Group (INAG), INAG Tech. Memorandum, available at: http://www.ursi.org/files/CommissionWebsites/INAG/web-73/confidence_score.pdf, 2013.
- Galkin, I. A.: Standard Archiving Output (SAO) Format, University of Massachusetts Lowell, 600 Suffolk Street, Lowell, MA 01854, USA, available at: <ftp://ftp.ngdc.noaa.gov/STP/ionosonde/documentation/SAO%20version%204.2.pdf>, 2006.
- Galkin, I. A. and Reinisch, B. W.: The new ARTIST 5 for all digisondes, *Ionosonde Network Advisory Group Bulletin*, 69, 1–8, available at:
10 <http://www.ursi.org/files/CommissionWebsites/INAG/web-69/2008/artist5-inag.pdf>, 2008.
- Hernández-Pajares, M., Juan, J. M., Sanz, J., Orus, R., Garcia-Rigo, A., Feltens, J., Komjathy, A., Schaer, S. C., and Krankowski, A.: The IGS VTEC maps: a reliable source of ionospheric information since 1998, *J. Geodesy*, 83, 263–275, <https://doi.org/10.1007/s00190-008-0266-1>, 2009.
- Huang, X. and Reinisch, B. W.: Vertical electron content from ionograms in real time, *Radio Sci.*, 36, 335–342,
15 <https://doi.org/10.1029/1999RS002409>, 2001.
- Jakowski, N.: Ionospheric GPS radio occultation measurements on board CHAMP, *GPS Solut.*, 9, 88–95, <https://doi.org/10.1007/s10291-005-0137-7>, 2005.
- Jiang, C., Yang, G., Lan, T., Zhu, P., Song, H., Zhou, C., Cui, X., Zhao, Z., and Zhang, Y.: Improvement of automatic scaling of vertical incidence ionograms by simulated annealing, *J. Atmos. Sol-Terr. Phy.*, 133, 178–184, <https://doi.org/10.1016/j.jastp.2015.09.002>, 2015.
- 20 Jin, S. and Jin, R.: GPS Ionospheric Mapping and Tomography: A case of study in a geomagnetic storm, in: *Proceeding of IEEE Int. Geosci. and Remote Se.*, Vancouver, Canada, 24–29 July 2011, pp. 1127–1130, 2011.
- Klipp, T. S., Petry, A., Souza, J. R., Falcão, G. S., Velho, H. F. C., Paula, E. R., Antreich, F., Hoque, M., Kriegel, M., Berdermann, J., Jakowski, N., Fernandez-Gomez, I., Borries, C., Sato, H., and Wilken, V.: Evaluation of Ionospheric Models for Central and South Americas, *Adv. in Space Res.*, in review, 2019.
- 25 Pezzopane, M. and Scotto, C.: Automatic scaling of critical frequency foF2 and MUF (3000) F2: A comparison between Autoscala and ARTIST 4.5 on Rome data, *Radio Sci.*, 42, RS4003, <https://doi.org/10.1029/2006RS003581>, 2007.
- Reinisch, B. and Huang, X.: Deducing topside profiles and total electron content from bottomside ionograms, *Adv. in Space Res.*, 27, 23 – 30, [https://doi.org/10.1016/S0273-1177\(00\)00136-8](https://doi.org/10.1016/S0273-1177(00)00136-8), 2001.
- Reinisch, B., Huang, X., Galkin, I., Paznukhov, V., and Kozlov, A.: Recent advances in real-time analysis of ionograms and ionospheric drift
30 measurements with digisondes, *J. Atmos. Sol-Terr. Phy.*, 67, 1054 – 1062, <https://doi.org/10.1016/j.jastp.2005.01.009>, 2005.
- Reinisch, B. W. and Galkin, I. A.: Global ionospheric radio observatory (GIRO), *Earth, Planets and Space*, 63, 377–381, 2011.
- Reinisch, B. W. and Xueqin, H.: Automatic calculation of electron density profiles from digital ionograms: 3. Processing of bottomside ionograms, *Radio Sci.*, 18, 477–492, <https://doi.org/10.1029/RS018i003p00477>, 1983.
- Schaer, S., Gurtner, W., and Feltens, J.: IONEX: The IONosphere Map EXchange Format Version 1, in: *Proceedings of the IGS AC workshop*, Darmstadt, Germany, 9–11 February 1998, pp. 233–247, 1998.
- 35 Scotto, C. and Pezzopane, M.: A software for automatic scaling of foF2 and MUF (3000) F2 from ionograms, in: *Proceedings of URSI XXVIIth General Assembly*, Maastricht, Holland, 17–24 August, 2002.



Scotto, C. and Pezzopane, M.: A method for automatic scaling of sporadic E layers from ionograms, *Radio Sci.*, 42, RS2012, <https://doi.org/10.1029/2006RS003461>, 2007.

5 Stankov, S., Jodogne, J.-C., Kutiev, I., Stegen, K., and Warnant, R.: Evaluation of the automatic ionogram scaling for use in real-time ionospheric density profile specification: Dourbes DGS-256/ARTIST-4 performance., *Annals of Geophysics*, 55, 283–291, <https://doi.org/10.4401/ag-4976>, 2012.



Table 1. Correspondent CS values for C-Level flags representation.

Confidence Score	C-level
81..100	11
61..80	22
41..60	33
21..40	44
0..20	55



Table 2. Ionosonde locations and correspondent closest IGS grid data location.

Ionosonde: Lat, Lon	Closest IGS data Lat, Lon
BVJ03: 2.8°, -60.7°	2.5°, -60.0°
CAJ2M: -22.7°, -45.0°	-22.5°, -45.0°
CGK21: -20.5°, -55.0°	-20.0°, -55.0°
FZA0M: -3.9°, -38.4°	-5.0°, -40.0°
SAA0K: -2.6°, -44.2°	-2.5°, -45.0°